Band Edge Electronic Structure of $BiVO_4$: Elucidating the Role of the Bi s and V d Orbitals

Aron Walsh,* Yanfa Yan, Muhammad N. Huda, Mowafak M. Al-Jassim, and Su-Huai Wei

National Renewable Energy Laboratory, Golden, Colorado 80401

Received October 23, 2008. Revised Manuscript Received December 11, 2008

We report the first-principles electronic structure of $BiVO_4$, a promising photocatalyst for hydrogen generation. $BiVO_4$ is found to be a direct band gap semiconductor, despite having band extrema away from the Brillouin zone center. Coupling between Bi 6s and O 2p forces an upward dispersion of the valence band at the zone boundary; however, a direct gap is maintained via coupling between V 3d, O 2p, and Bi 6p, which lowers the conduction band minimum. These interactions result in symmetric hole and electron masses. Implications for the design of ambipolar metal oxides are discussed.

Introduction

Metal oxides represent ideal catalysts for solar-driven hydrogen production and other photocatalytic applications due to their low cost and high stability in aqueous solution.[1−7] The major drawback is that most binary metal oxides suffer from band gaps too large (>3 eV) to absorb a significant fraction of visible light (e.g., TiO_2). For solar to hydrogen conversion efficiencies above 15%, which are needed to compete with direct photovoltaic driven electrolysis, a band gap below 2.2 eV is required.[8]

Typical metal oxides have valence and conduction bands composed of O 2p and metal s character, respectively (Figure 1). The high ionic character ensures a large separation between the band edges, for example, ZnO (3.4 eV[9]), Ga_2O_3 (4.5 eV[10]), and Al_2O_3 (8.8 eV[11]). One avenue to overcome this limitation is the use of transition metal cations with d^n electronic configurations; however, while absorption in the visible range is gained, for example, Fe_2O_3 (∼2.0 eV[12]) and Co_3O_4 (∼1.3 eV[13]), photogenerated carrier transport and extraction become problematic due to the small polaron

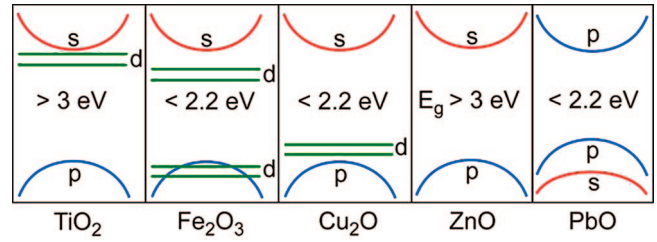

Figure 1. Illustrated distribution of the electronic states around the band edges in typical crystalline metal oxide frameworks.

dominated conductivity and associated high resistivity.[14,15] An alternative solution can be found from the choice of post-transition metal cations with occupied high binding energy s states, producing an O 2p metal p band gap, for example, PbO (2.1 eV[9,16]), SnO (2.4 eV[17,18]), and Bi_2O_3 (2.5 eV[9,19]). Indeed, the photocatalytic properties of PbO have been demonstrated with photogenerated currents of up to 4 mA/cm^2 under white light illumination.[20] The main issue arising from ns^2 cations is that coupling between the filled cation s and anion p states generally results in an unfavorable indirect band gap (e.g., PbO[21]) where band edge optical absorption varies with the square root of the photon energy. For direct gap semiconductors, these transitions are proportional to the photon energy squared. This requires thicker films for indirect materials, increasing the cost, and decreasing the carrier extraction efficiencies.

Consequently, it is becoming increasingly clear that to overcome the intrinsic limitations of binary metal oxides for next generation photocatalytic and optoelectronic applications, it will be necessary to combine multiple cations to

* Corresponding author. E-mail: aron_walsh@nrel.gov.

(1) Alexander, B. D.; Kulesza, P. J.; Rutkowska, I.; Solarska, R.; Augustynski, J. *J. Mater. Chem.* **2008**, *18*, 2298.
(2) Van de Krol, R.; Liang, Y.; Schoonman, J. *J. Mater. Chem.* **2008**, *18*, 2311.
(3) Woodhouse, M.; Herman, G. S.; Parkinson, B. A. *Chem. Mater.* **2005**, *17*, 4318.
(4) Woodhouse, M.; Parkinson, B. A. *Chem. Mater.* **2008**, *20*, 2495.
(5) Walsh, A.; Wei, S.-H.; Yan, Y.; Al-Jassim, M. M.; Turner, J. A.; Woodhouse, M.; Parkinson, B. A. *Phys. Rev. B* **2007**, *76*, 165119.
(6) Walsh, A.; Yan, Y.; Al-Jassim, M. M.; Wei, S.-H. J. *Phys. Chem. C* **2008**, *112*, 12044.
(7) Osterloh, F. E. *Chem. Mater.* **2008**, *20*, 35.
(8) Based on the reference Air Mass 1.5 spectra (http://rredc.nrel.gov/solar/spectra/am1.5) and 100% quantum efficiency.
(9) Madelung, O. M. *Semiconductors: Data Handbook*, 3rd ed.; Springer: Berlin, 2004.
(10) Schmitz, G.; Gassmann, P.; Franchy, R. *J. Appl. Phys.* **1998**, *83*, 2533.
(11) Perevalov, T.; Shaposhnikov, A.; Gritsenko, V.; Wong, H.; Han, J.; Kim, C. *JETP Lett.* **2007**, *85*, 165.
(12) Cornell, R. M.; Schwertmann, U. *The Iron Oxides*; VCH: Weinheim, 1996.
(13) Kim, K. J.; Park, Y. R. *Solid State Commun.* **2003**, *127*, 25.
(14) Cox, P. A. *The Electronic Structure and Chemistry of Solids*; Oxford University Press: New York, 1987.
(15) Morin, F. J. *Phys. Rev.* **1954**, *93*, 1195.
(16) Walsh, A.; Watson, G. W. *J. Solid State Chem.* **2005**, *178*, 1422.
(17) Walsh, A.; Watson, G. W. *Phys. Rev. B* **2004**, *70*, 235114.
(18) Geurts, J.; Rau, S.; Richter, W.; Schmitte, F. J. *Thin Solid Films* **1984**, *121*, 217.
(19) Dolocan, V. *Phys. Status Solidi A* **1978**, *45*, K155.
(20) Veluchamy, P.; Minoura, H. *Appl. Phys. Lett.* **1994**, *65*, 2431.
(21) Watson, G. W.; Parker, S. C.; Kresse, G. *Phys. Rev. B* **1999**, *59*, 8481.

10.1021/cm802894z CCC: $40.75
Published on Web 01/14/2009

form functionalized multiternary oxides.[3−5,22,23] Our recent and ongoing work has focused on combining transition metal $3d^n$ cations with ns^0 cations to produce ternary $Co_{3-x}Al_xO_4$ and related spinels.[5,6] An alternative route may be found through the combination of nd^0 (e.g., Ti 4^+, V 5^+, Nb 5^+) and ns^2 cations (e.g., Bi 3^+, Sn 2^+) producing ternary compounds such as $Bi_{20}TiO_{32}$,[24] $SnNb_2O_6$,[25] and $BiVO_4$.[26−28] $BiVO_4$ has shown particular promise for water photodecomposition with the presence of both a low band gap (2.4−2.5 eV)[26−28] and reasonable band edge alignment with respect to the water redox potentials.[29] It has been reported to exhibit both n- and p-type semiconducting properties,[30] in addition to high photon-to-current conversion efficiencies (>40%).[26,31]

To date, the fundamental electronic structure of $BiVO_4$ has not been well explored. In particular, it is unclear whether the band gap is direct or indirect and what role the occupied Bi 6s lone pair electrons[32−36] may play in determining the valence band edge positions and charge transport properties. Here we report the results of first-principles band structure calculations, which predict $BiVO_4$ to be a direct band gap semiconductor. In a centrosymmetric lattice, interaction between Bi 6s and O 2p results in an upward dispersion of the valence band away from Γ and a relatively light hole effective mass. In typical metal oxides, the s-like conduction band is centered at Γ, which would result in an undesirable indirect band gap; however, the presence of unoccupied V 3d states in $BiVO_4$, coupled with O 2p and Bi 6p levels, results in a conduction band minimum at the Brillouin zone edge, maintaining favorable low energy direct transitions.

Crystal Structure

$BiVO_4$ is known to exist in three polymorphs (orthorhombic pucherite,[37] tetragonal dreyerite,[38] and monoclinic clinobisvanite[38]); however, it is the thermodynamically stable clinobisvanite phase that exhibits good photoelectrochemical behavior.[26−28] The base centered monoclinic crystal structure (space group 15, C_{2h}^6) contains four unique lattice sites: Bi (4e), V (4e), O1 (8f), and O2 (8f).[38,39] By taking into account the crystal inversion symmetry, a primitive cell of two formula units can be constructed, Figure 2. The layered structure of Bi−V−O units stacked parallel to the *c* axis draws features from both the Bi_2O_3 and the V_2O_5 binary analogues.[33,40] The Bi coordination environment is a distorted oxygen octahedron, with nearest neighbor distances ranging from 2.35 to 2.53 Å, while V is at the center of a distorted tetrahedron with 2 × 1.74 Å and 2 × 1.75 Å bond lengths. O1 is coordinated to one Bi and V, while O2 is coordinated to two Bi and a single V. The stoichiometry of the system implies formal oxidation states of 3^+, 5^+, and 2^- for Bi ($5d^{10}6s^2$), V ($3d^0$), and O ($2p^6$), respectively. The $6s^2$ electronic configuration of Bi is associated with the sterically active lone pair commonly present with ns^2 valence cations (e.g., Pb 2^+, Sn 2^+, Sb 3^+),[16,32,36] a driving force for asymmetric coordination environments.

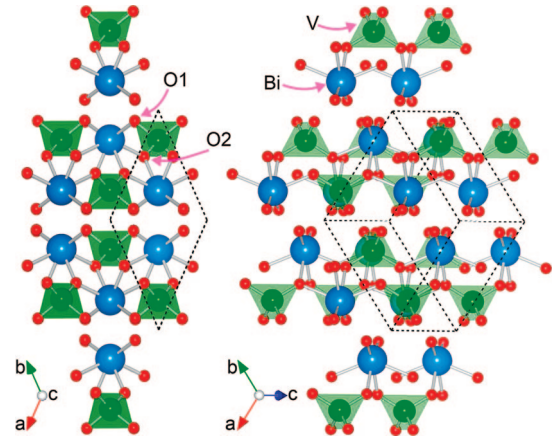

Figure 2. Representation of the crystal structure of $BiVO_4$ with blue, bismuth; red, oxygen; and green, vanadium tetrahedra. The base centered monoclinic primitive cell is indicated by the dashed black lines.

Calculation Methodology

Calculations were performed using density functional theory (DFT)[41,42] as implemented in the VASP[43,44] code. Three dimensional periodic boundary conditions were used to approximate an infinite solid.[45] Exchange-correlation effects were described through the generalized gradient approximation, within the Perdew-Burke-Ernzerhof (PBE)[46] formalism. The core electrons (Bi:[Xe], V:[Ne], O:[He]) were treated within the projector augmented wave (PAW) method.[47] The *k*-point density (8 × 8 × 8) and plane wave cutoff threshold (500 eV) were found to be well converged; the equilibrium volume was obtained through minimization of the stress tensor at an elevated cutoff of 750 eV. Both the optical transition matrix

(22) Zhu, Y. Z.; Chen, G. D.; Ye, H.; Walsh, A.; Moon, C. Y.; Wei, S.-H. *Phys. Rev. B* **2008**, *77*, 245209.
(23) Da Silva, J. L. F.; Yan, Y.; Wei, S.-H. *Phys. Rev. Lett.* **2008**, *100*, 255501.
(24) Kong, L.; Chen, H. Y.; Hua, W.; Zhang, S.; Chen, J. P. *Chem. Commun.* **2008**, 4977.
(25) Hosogi, Y.; Shimodaira, Y.; Kato, H.; Kobayashi, H.; Kudo, A. *Chem. Mater.* **2008**, *20*, 1299.
(26) Sayama, K.; Nomura, A.; Arai, T.; Sugita, T.; Abe, R.; Yanagida, M.; Oi, T.; Iwasaki, Y.; Abe, Y.; Sugihara, H. *J. Phys. Chem. B* **2006**, *110*, 11352.
(27) Luo, H.; Mueller, A. H.; McCleskey, T. M.; Burrell, A. K.; Bauer, E.; Jia, Q. X. J. *Phys. Chem. C* **2008**, *112*, 6099.
(28) Kudo, A.; Omori, K.; Kato, H. *J. Am. Chem. Soc.* **1999**, *121*, 11459.
(29) Long, M. C.; Cai, W. M.; Kisch, H. J. *Phys. Chem. C* **2008**, *112*, 548.
(30) Vinke, I. C.; Diepgrond, J.; Boukamp, B. A.; de Vries, K. J.; Burggraaf, A. J. *Solid State Ionics* **1992**, *57*, 83.
(31) Sayama, K.; Nomura, A.; Zou, Z.; Abe, R.; Abe, Y.; Arakawa, H. *Chem. Commun.* **2003**, 2908.
(32) Payne, D. J.; Egdell, R. G.; Walsh, A.; Watson, G. W.; Guo, J.; Glans, P. A.; Learmonth, T.; Smith, K. E. *Phys. Rev. Lett.* **2006**, *96*, 157403.
(33) Walsh, A.; Watson, G. W.; Payne, D. J.; Edgell, R. G.; Guo, J. H.; Glans, P. A.; Learmonth, T.; Smith, K. E. *Phys. Rev. B* **2006**, *73*, 235104.
(34) Walsh, A.; Watson, G. W. *Chem. Mater.* **2007**, *19*, 5158.
(35) Walsh, A.; Watson, G. W.; Payne, D. J.; Atkinson, G.; Egdell, R. G. *J. Mater. Chem.* **2006**, *16*, 3452.
(36) Stoltzfus, M. W.; Woodward, P. M.; Seshadri, R.; Klepeis, J. H.; Bursten, B. *Inorg. Chem.* **2007**, *46*, 3839.
(37) Qurashi, M. M.; Barnes, W. H. *Am. Mineral.* **1953**, *37*, 423.
(38) Sleight, A. W.; Chen, H. Y.; Ferretti, A.; Cox, D. E. *Mater. Res. Bull.* **1979**, *14*, 1571.
(39) Liu, J. C.; Chen, J. P.; Li, D. L. *Acta Phytophysiol. Sin.* **1983**, *32*, 1053.
(40) Scanlon, D. O.; Walsh, A.; Morgan, B. J.; Watson, G. W. *J. Phys. Chem. C* **2008**, *112*, 9903.
(41) Hohenberg, P.; Kohn, W. *Phys. Rev.* **1964**, *136*, B864.
(42) Kohn, W.; Sham, L. J. *Phys. Rev.* **1965**, *140*, A1133.
(43) Kresse, G.; Furthmüller, J. *Comput. Mater. Sci.* **1996**, *6*, 15.
(44) Kresse, G.; Furthmüller, J. *Phys. Rev. B* **1996**, *54*, 11169.
(45) Payne, M. C.; Teter, M. P.; Allan, D. C.; Arias, T. A.; Joannopoulos, J. D. *Rev. Mod. Phys.* **1992**, *64*, 1045.
(46) Perdew, J. P.; Burke, K.; Ernzerhof, M. *Phys. Rev. Lett.* **1996**, *77*, 3865.
(47) Blöchl, P. E. *Phys. Rev. B* **1994**, *50*, 17953.

Table 1. Equilibrium Structural Parameters of Monoclinic $BiVO_4$ Derived from Experiment[39] and PBE-DFT Calculations[a]

	experiment[39]	calculations
a (Å)	7.253	7.299 (+0.6%)
b (Å)	11.702	11.769 (+0.6%)
c (Å)	5.096	5.145 (+1.0%)
β (deg)	134.23	134.26

[a] The percentage deviations are shown in parenthesis.

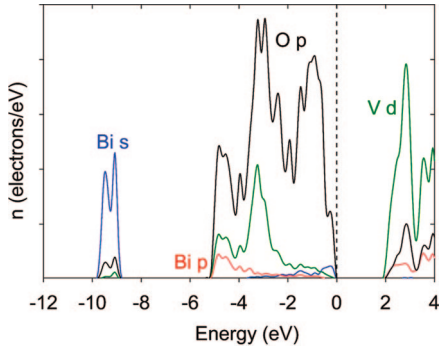

Figure 3. Ion-projected electronic density of states. The highest occupied state is set to 0 eV (dashed vertical line).

elements and optical absorption spectrum were calculated within the transversal approximation and the PAW method.[48] Structure and charge density visualization and analysis were performed using VESTA.[49]

Results and Discussion

The equilibrium structural parameters are in very good agreement with experiment,[39] with deviations of less than 1% in the lattice constants, Table 1. Three pairs of Bi−O bond lengths are found at 2.445, 2.473, and 2.475 Å, while two pairs of V−O bond lengths are found at 1.738 and 1.749 Å.

The ion-projected valence electronic densities of states (DOS) are plotted in Figure 3. The main O 2p based valence band is spread between 0 and −5 eV, with respect to the highest occupied state. An additional peak is found at −9.5 eV consisting of the majority of Bi 6s states. These features are consistent with previous calculations[26,36] and X-ray photoemission measurements.[26] As a result of its elevated oxidation state and formal d^0 configuration, V makes only a small contribution to the valence density of states, but hybridization with O 2p, centered at −3.5 eV, is observed. Closer inspection of the O 2p valence band indicates the presence of Bi 6s and Bi 6p states at the top and bottom, respectively. This is consistent with previous analysis of Bi_2O_3, where coupling between Bi 6s and O 2p produces antibonding Bi 6s states toward the top of the valence band,[33] and the distribution of states is hypothesized for $BiVO_4$ on the basis of excitation and emission spectra.[28] While an isolated O 2p valence band is resilient to oxidation, the presence of antibonding cation−anion electronic states at lower binding energy is beneficial for hole formation and mobility, as demonstrated by the excellent p-type behavior

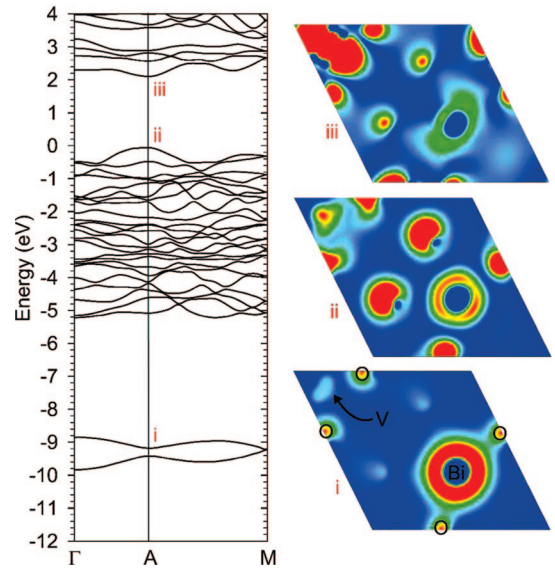

Figure 4. Electronic band structure along the Γ−A−M lines. The highest occupied state is set to 0 eV. Charge density contour plots through a (001) plane are shown for three bands at the A point (plotted from 0 (blue) to 0.01 (red) $e \cdot Å^{-3}$).

of both Cu_2O[50] and SnO.[51] The conduction band is found to be dominated by V 3d states, with significant contributions from O 2p and Bi 6p also present.

The band structure, drawn along two high symmetry lines[52] of the Brillouin zone, is shown in Figure 4. $BiVO_4$ is found to be a direct band gap insulator. While the PBE-DFT band gap of 2.16 eV is marginally underestimated relative to experiment (2.4−2.5 eV), the difference is much less than metal oxides with s-like conduction bands such as ZnO (where the error exceeds 2 eV).[53,54] The valence and conduction band extrema are found away from the gamma point where the strength of interatomic hybridization within the Bi−V−O layers is increased. While there is some curvature at the band edges, the high densities of states around the band gap mean that the bands are far from parabolic and are therefore not expected to be well described under a typical semiconductor effective mass approximation. However, fitting the energy-momentum dependence of the states along the A−M line predicts effective masses on the order of 0.3 m_e for both holes and electrons; in metal oxides the hole masses are typically much heavier, for example, 16 m_e for In_2O_3.[55] Such light masses should facilitate efficient photoexcited charge carrier separation and extraction.

To gain a deeper understanding of the band structure features, we have plotted projections of the wave function for three specific bands at the A point through a (001) plane containing both Bi and V atoms, labeled i, ii, and iii in Figure 4. The first projection at −9.1 eV is of predominately Bi 6s character, as expected from the corresponding DOS in this

(48) Gajdos, M.; Hummer, K.; Kresse, G.; Furthmuller, J.; Bechstedt, F. *Phys. Rev. B* **2006**, *73*, 045112.
(49) Momma, K.; Izumi, F. *J. Appl. Crystallogr.* **2008**, *41*, 653.
(50) Nie, X.; Wei, S.-H.; Zhang, S. B. *Phys. Rev. Lett.* **2002**, *88*, 066405.
(51) Ogo, Y.; Hiramatsu, H.; Nomura, K.; Yanagi, H.; Kamiya, T.; Hirano, M.; Hosono, H. *Appl. Phys. Lett.* **2008**, *93*, 032113.
(52) Aroyo, M. I.; Kirov, A.; Capillas, C.; Perez-Mato, J. M.; Wondratschek, H. *Acta Crystallogr., Sect. A* **2006**, *62*, 115.
(53) Janotti, A.; Van de Walle, C. G. *Phys. Rev. B* **2007**, *76*, 165202.
(54) Lany, S.; Zunger, A. *Phys. Rev. B* **2008**, *78*, 235104.
(55) Walsh, A.; Da Silva, J. L. F.; Wei, S.-H. *Phys. Rev. B* **2008**, *78*, 075211.

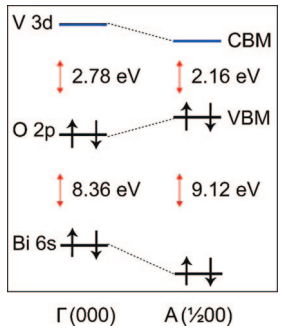

Figure 5. Schematic orbital level interactions derived from the calculated band structure of $BiVO_4$.

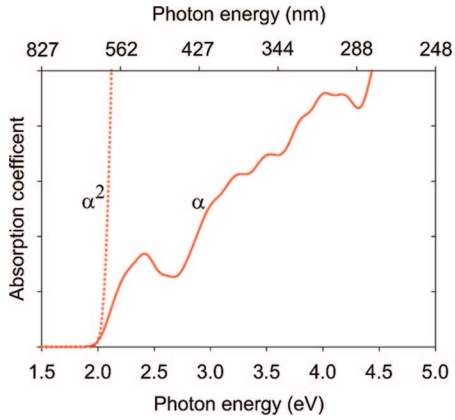

Figure 6. Calculated optical absorption spectrum of $BiVO_4$ summed over all possible direct valence to conduction band transitions.

energy range; however, significant hybridization between Bi and the neighboring O (which lies slightly out of plane) can also be observed. The second projection at 0 eV is dominated by Bi and O character. Here the density node between Bi and O is suggestive of the antibonding nature of their interaction. As a result of the role of symmetry and orbital phase constraints, Bi 6s−O 2p coupling does not occur at the gamma point, which results in the upward dispersion toward A, where this interaction is maximized. The final projection is of the conduction band minimum state, which contains contributions from V 3d, O 2p, and Bi 6p. The resulting energy level interactions are summarized in Figure 5. At the gamma point, the valence and conduction band extrema contain contributions solely from O 2p and V 3d, respectively. Away from the zone center, coupling with Bi 6s (valence band) and Bi 6p/O 2p (conduction band) is observed. Quantitatively, the Bi 6s−O 2p interaction results in an energy raise of 0.4 eV in the valence band maximum.

The corresponding calculated optical absorption spectrum is shown in Figure 6. Fundamental band-edge transitions are dipole allowed, with absorption beginning at the band gap threshold (2.1 eV), which results in a peak centered around 2.4 eV before a continued ascent to shorter photon wavelengths. The same onset feature has been observed experimentally in the UV−vis absorption spectrum.[27] The slow rise in the absorption coefficient, resulting from a range of weak valence to conduction band transitions, would suggest significant transmission in the visible range (an inefficient use of low energy photons), and therefore even from the viewpoint of a perfect bulk crystal, there is significant scope for improving oxide photocatalytic properties beyond $BiVO_4$.

Drawing from our present results it is clear that the combination of multiple cations to form complex oxides can be used to influence the ground-state electronic structure and associated optical absorption. The key question that needs to be addressed is what combination of cations will be optimal. Exhaustive enumeration of all possible multiternary cation combinations is impossible, and hence intuitive guidance is imperative for future success. For photocatalysis, it has been consistently shown that the presence of nd^0 ions (e.g., Ti 4^+, V 5^+, W 6^+), where the localized nature of the cation d conduction band is extended through hybridization with O 2p to produce large polaron carriers,[56] is beneficial as catalytic redox centers. While the delocalized conduction bands of ns^0 cations (Zn 2^+, Ga 3^+, Sn 4^+) are desirable for enhanced conductivity, all attempts to reduce their otherwise too large band gaps have failed to produce a catalytically active material with photocurrents at the mA/cm^2 scale; recombination of photogenerated carriers dominates. Unfortunately, the direct combination of nd^0 and ns^0 cations generally maintains the large band gaps of the component oxides, for example, Zn_2TiO_4 (3.7 eV[57]) and $CdTiO_3$ (3.7 eV[58]); their high transmission of visible light make them better suited for application as transparent conductors.

To raise the valence band level and hence reduce the band gap of metal oxides, three options remain open: (i) anion substitution with less electronegative species (e.g., N or S) producing lower binding energy anion p states; (ii) inclusion of cations with occupied low binding energy d states such as Cu or Ag (nd^{10}); and (iii) inclusion of cations with occupied low binding energy s states such as Bi or Sn (ns^2). The first approach has been proven inherently problematic; isovalent chalcogenide (S_O, Se_O, Te_O) doping of metal oxides is unstable in solution, while uncompensated aliovalent doping (N_O + hole) is detrimental to the generated photocurrent through reduced crystallinity and enhanced carrier recombination.[59] An alternative route for anion incorporation attracting recent attention is the formation of multiternary metal oxynitride or oxysulfide compounds.[60,61] The second approach can result in the compositional flexibility of a homologous series of compounds such as the Cu and Ag delafossite ternary ABO_2 oxides, where A = Cu or Au and B is a trivalent cation.[50,62,63] For the third approach, no homologous series are found due to the strong preference of ns^2 cations for disordered coordination and hence unique crystal structures that vary with the cation s binding energy.

(56) Breckenridge, R. G.; Hosler, W. R. *Phys. Rev.* **1953**, *91*, 793.
(57) Mayen-Hernandez, S. A.; Torres-Delgado, G.; Castanedo-Perez, R.; Villarreal, M. G.; Cruz-Orea, A.; Alvarez, J. G. M.; Zelaya-Angel, O. J. *Mater. Sci: Mater. Electron.* **2007**, *18*, 1127.
(58) Mayén-Hernández, S. A.; Torres-Delgado, G.; Castanedo-Pérez, R.; Cruz-Orea, A.; Mendoza-Alvarez, J. G.; Zelaya-Angel, O. *Sol. Energy Mater. Sol. Cells* **2006**, *90*, 2280.
(59) Ahn, K.-S.; Yan, Y.; Shet, S.; Deutsch, T.; Turner, J.; Al-Jassim, M. M. *Appl. Phys. Lett.* **2007**, *91*, 231909.
(60) Wang, X.; Maeda, K.; Lee, Y.; Domen, K. *Chem. Phys. Lett.* **2008**, *457*, 134.
(61) Yashima, M.; Lee, Y.; Domen, K. *Chem. Mater.* **2007**, *19*, 588.
(62) Kawazoe, H.; Yasukawa, M.; Hyodo, H.; Kurita, M.; Yanagi, H.; Hosono, H. *Nature* **1997**, *389*, 939.
(63) Sheets, W. C.; Stampler, E. S.; Bertoni, M. I.; Sasaki, M.; Marks, T. J.; Mason, T. O.; Poeppelmeier, K. R. *Inorg. Chem.* **2008**, *47*, 2696.

The viability of both cation approaches has been made apparent in a recent optical evaluation of ternary tungstenates,[64] which found $SnWO_4$ and $CuWO_4$ to be the only XWO_4 nontransition metal oxides with optical band gaps lower than 2.5 eV. Both the raise in valence band energy and the added dispersion of the ns^2 and nd^{10} cations are a characteristic that should be exploited in future material exploration. Of particular benefit is the lighter hole mass and antibonding character at the top of the valence band, which can be tuned to obtain p-type hole conducting and ambipolar metal oxides, two highly elusive material classes.

Conclusion

In summary, we have presented a first-principles electronic structure analysis of $BiVO_4$. Through examining the electronic density of states and band structure, we can understand why $BiVO_4$ is a promising photocatalyst for hydrogen generation. $BiVO_4$ is found to be a direct band gap semiconductor, despite having band extrema away from the Brillouin zone center. Coupling between Bi 6s and O 2p forces an upward dispersion of the valence band at the zone boundary; however, a direct gap is maintained via coupling among V 3d, O 2p, and Bi 6p, which lowers the conduction band minimum. These interactions result in symmetric hole and electron masses. However, from examination of bulk optical absorption, improvements are possible, and we suggest that future work should closely consider the combination of nd^0 and ns^2/nd^{10} cations for both reducing the oxide band gaps and increasing the hole conductivity.

Acknowledgment. This work is supported by the U.S. Department of Energy (DOE) under Contract No. DE-AC36-08GO28308. Computing resources of the National Energy Research Scientific Computing Center were employed, which is supported by DOE under Contract No. DE-AC02-05CH11231.

CM802894Z

(64) Lacomba-Perales, R.; Ruiz-Fuertes, J.; Errandonea, D.; Martínez-García, D.; Segura, A. *Euro Phys. Lett.* **2008**, *83*, 37002.